

Rover-Based Surface and Subsurface Modeling for Planetary Exploration

Paul Furgale, Tim Barfoot, and Nadeem Ghafoor

Abstract We develop and test a technique for the creation of coupled surface and subsurface models. Images from a stereo camera are used to estimate the motion of a rover that is collecting ground penetrating radar (GPR) data. The motion estimate and raw sensor data are used to build two novel data products: (1) A three-dimensional, photorealistic surface model coupled with a ribbon of GPR data, and (2) a two-dimensional, topography-corrected GPR radargram with the reconstructed surface topography plotted above. Each result is derived from only the onboard sensors of the rover, as would be required in a planetary exploration setting. These techniques were tested using data collected in a Mars analogue environment on Devon Island in the Canadian High Arctic. GPR transects were gathered over polygonal patterned ground similar to that seen by the Phoenix lander on Mars. Using the techniques developed here, scientists may remotely explore the interaction of the surface topography and subsurface structure as if they were on site.

1 Introduction

The use of ground penetrating radar (GPR) together with a stereo camera on planetary exploration rovers has been proposed several times [1, 7] and is now in development for the European Space Agency's (ESA) ExoMars project (2014) [22]. Used together, surface and subsurface imaging will aid in the search for liquid water and evidence of life. The ESA mission proposes using the stereo camera for site selection and survey, while the GPR will then be used to characterize the subsurface stratigraphy, and to select sites for drilling.

Paul Furgale, Tim Barfoot
University of Toronto Institute for Aerospace Studies,
e-mail: {paul.furgale,tim.barfoot}@utoronto.ca

Nadeem Ghafoor
MDA Space Missions, Toronto e-mail: Nadeem.Ghafoor@mdacorporation.com

Despite this interest, there are still several open issues regarding the use of GPR on a rover platform:

1. Rovers must be able to deliver information about the surface (topography, substrate particle size distribution, and/or the presence of any existing outcrops) that enables the operator to give local geologic context to the subsurface data. The location of the GPR traverse must be known with respect to the surface data captured by the rover, so that the scientific interpretation of the data is as close as possible to a direct (human) site survey.
2. For a more complete interpretation of GPR data, the radargram (i.e., the two-dimensional subsurface profile) should be corrected for topography (e.g., [15]). As planetary exploration rovers have no access to a global positioning system (GPS) equivalent, topographic profiles must be generated using other onboard sensors.
3. A flight-ready GPR antenna must satisfy size, mass and power consumption constraints and the integration must minimize interference from the rover's motors and metal chassis.

This paper addresses items 1 and 2 by using stereo imagery to enhance the GPR data. Stereo cameras have been deployed on the Mars Exploration Rovers and are planned for both the Mars Science Laboratory (2011) and the ExoMars Mission (2014) [22]. Visual odometry (VO)[17, 20, 3, 11]—full 6-degree-of-freedom motion estimation using a stereo camera as the primary sensor—is central to the work described in this paper. Our visual odometry algorithm produces motion estimates with accuracy between 0.5% and 5.3% of distance traveled.

On Earth, producing a site survey using GPR on rough terrain involves several manual steps:

1. Place fiduciary markers (e.g., flags) along the intended transect and survey their locations (e.g., using differential global positioning (DGPS)).
2. Drag the antenna along the transect at a constant speed to collect many GPR traces, manually inserting a mark into the data to note the time at which the antenna passes each fiduciary marker.
3. Linearly interpolate these manually-generated markers to correct the horizontal spacing of the GPR traces along the transect.
4. If the surface is not flat, correct the vertical offset of the GPR traces using surface topography manually collected with a DGPS (Step 1).
5. Concatenate the corrected traces into a raster image called a *radargram*.

Our technique uses a VO estimate to fully automate this procedure. Further, we produce two novel data products that may be used to explore the interaction of surface topography and subsurface structure: (1) A three-dimensional, photorealistic surface model coupled with a ribbon of GPR data, and (2) a two-dimensional, topography-corrected GPR radargram with the reconstructed surface topography plotted above.

These techniques have been tested using data gathered at two sites near the Haughton-Mars Project Research Station (HMPRS) on Devon Island, Nunavut, Canada. The sites exhibit polygonally patterned ground, a periglacial landform often

indicative of subsurface ice deposits [16]. Stereo images were captured during GPR transects and our integrated surface/subsurface modeling techniques were applied to the resulting data.

The rest of the paper is organized as follows. Our coupled surface and subsurface modeling system is described in Section 2. Sections 3 and 4 outline our field tests on Devon Island and the associated results. Our conclusions are provided in Section 5.

2 Integrated Surface and Subsurface Modeling

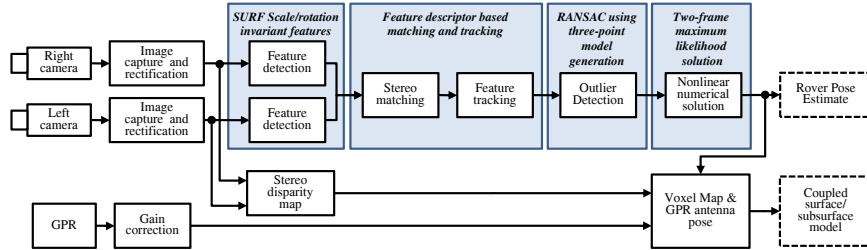


Fig. 1 An overview of the major processing blocks of our system.

This section will describe our integrated surface/subsurface modeling system. Data flow through the main processing blocks of our system can be seen in Figure 1. The images captured from a calibrated stereo camera are first undistorted and rectified. This process accounts for lens distortion and aligns the images as if they came from perfect pinhole cameras with parallel optical axes.

Our algorithm uses Speeded-Up Robust Features (SURF)—an algorithm to detect and describe scale-and-rotation-invariant features [4]—for both *matching* (across stereo pairs) and *tracking* (over time). This is a class of feature pioneered by Lowe [14]. Lowe’s Scale-Invariant Feature Transform (SIFT) algorithm has been used previously for object recognition [14], simultaneous localization and mapping [6], and visual odometry [3]. SURF is a similar algorithm that is much faster to compute because it uses integral images to approximate the operations used by SIFT to find and describe features. After two consecutive stereo pairs have been matched, features are tracked between frames. Feature descriptor matches between the consecutive left images are used as candidate tracks. We use a version of RANSAC [5] to simultaneously reject outlier feature tracks and produce a coarse motion estimate that is used to initialize our maximum likelihood solution.

Our maximum likelihood solution is similar to the one developed by Matthies [18] and deployed on the Mars Exploration Rovers [17]. At each timestep, N tracked features pass the outlier rejection stage. For each feature i , we triangulate the three-dimensional location of the point in each of the two consecutive stereo images. This results in a pair of points \mathbf{p}_1^{i1} and \mathbf{p}_2^{i2} . As the world is assumed to be rigid, we now

seek the rotation \mathbf{C}_{12} and translation ρ_1^{21} that align these two point clouds. This results in the objective function, J , which we seek to minimize:

$$J(\mathbf{C}_{12}, \rho_1^{21}) := \frac{1}{2} \sum_{i=1}^N (\mathbf{p}_1^{i1} - (\mathbf{C}_{12}\mathbf{p}_2^{i2} + \rho_1^{21}))^T \mathbf{W}_i (\mathbf{p}_1^{i1} - (\mathbf{C}_{12}\mathbf{p}_2^{i2} + \rho_1^{21})) \quad (1)$$

where \mathbf{W}_i is a weighting matrix. We use the inverse covariance of $\varepsilon_i := \mathbf{p}_1^{i1} - (\mathbf{C}_{12}\mathbf{p}_2^{i2} + \rho_1^{21})$ for \mathbf{W}_i , and thus J is a Mahalanobis distance, and finding the variables that minimize J also maximizes the joint likelihood of all the data. For further details, please refer to [8].

The motion estimates between each consecutive pair of images are then stacked up to give an estimate of the rover's entire traverse. As the robot is rigid, we obtain the transformation from the camera frame to the GPR frame through calibration, and so the visual odometry estimate also gives us the position of the GPR at each point along the traverse. Knowing the position of the camera and the GPR, we can transform all of the raw data into a common coordinate frame, \mathcal{F}_0 . This gives us the following intermediate data products, all expressed in \mathcal{F}_0 :

1. an estimate of the rover's position for each stereo image,
2. the sparse points used to compute the motion estimate,
3. larger point clouds for each stereo image obtained from dense stereo processing,
4. the position of the GPR at each data collection point.

These intermediate results are used to build the higher-level data products described below.

2.1 Three-Dimensional Surface and Subsurface Model

The first data product is a photorealistic, three-dimensional model of the surface, coupled with a model of the subsurface. Point sets derived from dense-stereo processing are aligned using the VO motion estimate [21]. The resulting point cloud is meshed and mapped with texture from the original images [2]. The GPR scan is modeled as a ribbon running under the surface mesh. The known transformation between the stereo camera and the GPR antenna is used to couple the surface and subsurface models. The resulting coupled model allows geologists to inspect a three-dimensional representation of the transect and explore the interaction of the surface morphology and the subsurface scan.

2.2 Two-Dimensional Topography-Corrected Radargram

The second data product is a two-dimensional, topography corrected radargram. The position and attitude of the antenna at each GPR trace is interpolated from the VO

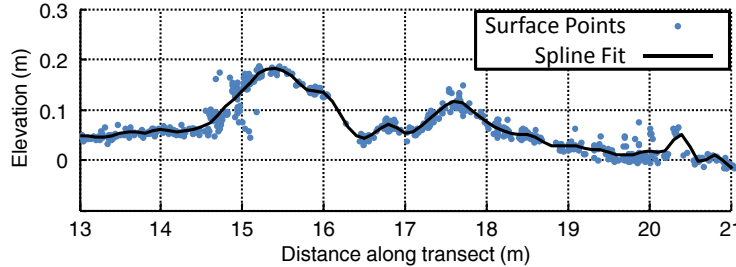


Fig. 2 Sparse surface points and the spline fit along the GPR antenna's path. This section is a polygon trough from transect *poly-2AS-1*.

estimate. This estimate is used in place of the DGPS survey to perform both the horizontal correction and the vertical correction. The profile of the surface below the antenna is estimated by fitting a spline to feature locations along the transect as shown in Figure 2. The spline improves on the topographic correction as it is able to capture narrow features over which the rover may drive.

3 Field testing

The experiments described in this paper were conducted on Devon Island in the Canadian High Arctic, as part of the Haughton-Mars Project. The Haughton-Mars Project Research Station (HMPRS) is situated just outside the northwest area of the Haughton impact crater, which is located at 75°22' N latitude and 89°41' W longitude. Our experiments were conducted approximately 10 kilometers northeast of HMPRS near Lake Orbiter. This site was selected based on ongoing research into the polygonal terrain it hosts. Image sequences from the stereo camera and GPR data were logged at two sites:

1. The Lake Orbiter Transects: Five straight-line transects were taken at the Lake Orbiter site (Figure 3(a)). Each transect is approximately 60 meters long.
2. The Mock Rover Transect: One transect, approximately 357 meters long, at a site that had not been previously studied (Figure 3(b)).

In our experiments, a rover was simulated using a pushcart equipped with rover engineering sensors (i.e., stereo camera, inclinometers, sun sensor, wheel odometers), a ground-penetrating radar, an on-board computer, and two independent GPS systems (one Real-Time Kinematic) used for ground-truth positioning (see Figure 4). Although this was not an actuated rover, our focus in this work is on problems of estimation, and thus it was entirely sufficient as a means to gather data. The GPR (and cart) we used was a Sensors&Software Noggin 250 MHz system [1]. Efforts were made to minimize the effect of the rover body on the GPR data quality (e.g., using plastic parts where possible). The stereo camera was a Point Gray

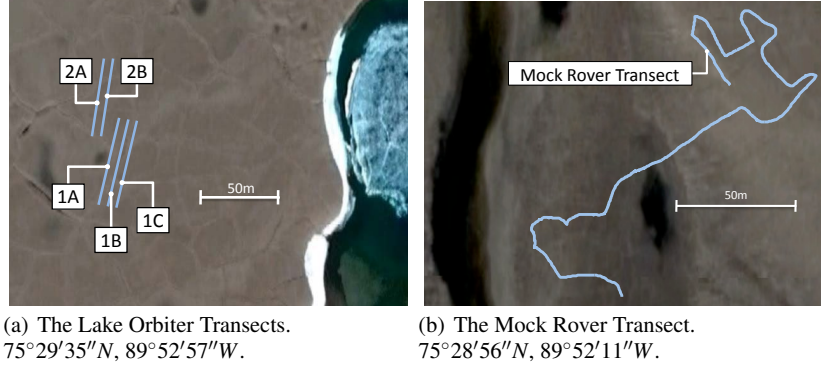


Fig. 3 Locations and transects on Devon Island, Nunavut, Canada used for field testing our integrated surface/subsurface modeling technique.

Research Bumblebee XB3 with a 24 cm baseline and 70° field of view, mounted approximately 1 m above the surface pointing downward by approximately 20°. Each image of the stereo pair was captured at 1280 × 960 pixel resolution.

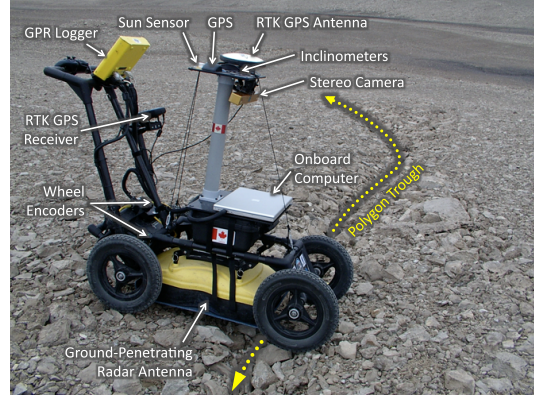


Fig. 4 The rover platform used for field testing.

4 Results

The visual odometry algorithm described in Section 2 was used to process all data collected at the Lake Orbiter site. We used a real-time kinematic GPS unit as ground-truth for our motion estimate. We determine the initial heading through a least-squares fit of the estimated track to the GPS for a small number of poses at the start

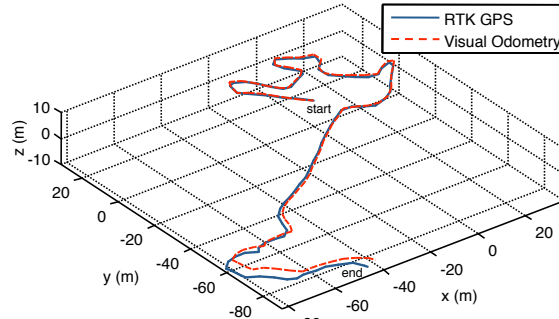


Fig. 5 Track plots of GPS and the VO estimate for the 357 meter Mock Rover Transect.

Table 1 Visual Odometry motion estimate results.

Transect	Distance Traveled (m)	Linear Error (m)	Percent Error	Number of Images
Mock Rover	357.30	5.83	1.63%	4818
poly-1AS-1	54.23	2.87	5.29%	333
poly-1BN-1	59.63	0.68	1.14%	316
poly-1BS-1	60.06	1.24	2.06%	317
poly-1CN-1	60.67	1.98	3.26%	327
poly-2AN-1	51.49	1.04	2.01%	270
poly-2AS-1	50.16	0.25	0.51%	263
poly-2BN-1	49.47	1.16	2.34%	260
poly-2BS-1	49.05	0.96	1.96%	258

of the traverse. These poses are then discarded and are not used when evaluating the linear position error. This is similar to the method used by [19].

The results are shown in Table 1, which lists the distance traveled and errors for all datasets collected. On the short Lake Orbiter transects (50 to 60 meters), position errors ranged from 0.5% to 5.3% of distance traveled. The results of the estimation on the Mock Rover Transect are plotted in Figure 4. This estimate accumulated 1.63% position error over this 357.3 meter traverse.

Our results approach those reported by other frame-to-frame VO algorithms [10, 20], and we believe this class of algorithm is suitable for applications such as this, which require a motion estimate over a short distances. To use VO over longer distances, the work of Konolige et al. offers insights into increasing performance, albeit at the cost of increased computational complexity [11].

4.1 Coupled Surface/Subsurface models

The complete coupled surface/subsurface model of the Mock Rover Transect is shown in Figure 6. The texture-mapped triangle mesh of the surface is displayed above the ribbon of GPR data. The model may be inspected using a Virtual Reality Modeling Language viewer and rendered from any viewpoint.

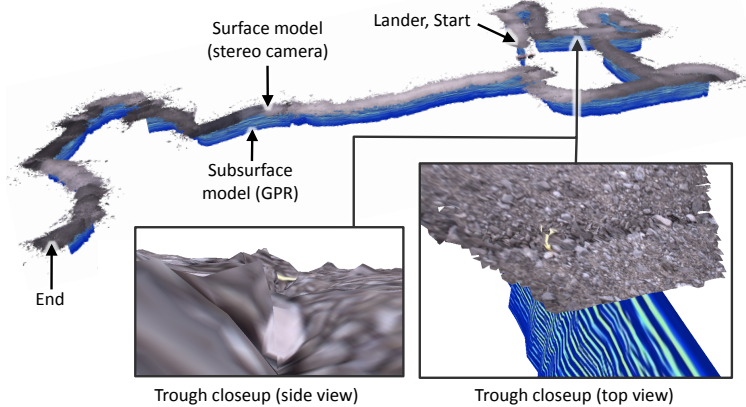


Fig. 6 Screenshots of the coupled surface/subsurface model.

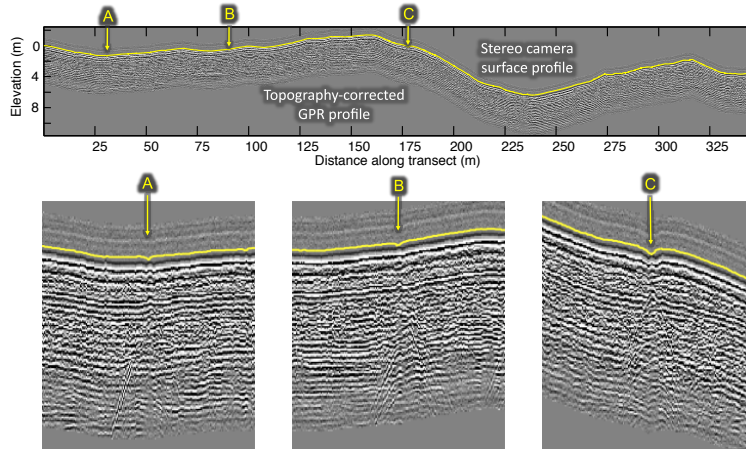


Fig. 7 GPR transect corrected for topography with surface profile plotted above.

Polygonal terrain—a network of interconnected trough-like depressions in the ground—is a landform commonly found throughout the polar regions of both Earth [13] and Mars [12]. In terrestrial environments, these features are often indicative of subsurface ice bodies termed ice wedges [16]. As noted by Hinkel et al. [9], ice wedges “produce exceedingly complex, high amplitude hyperbolic reflections” (p.187) due to the conical shape of the emitted GPR pulse. As a result, while ice wedges themselves are roughly triangular in shape—wider at the top and progressively narrowing with depth—their appearance on a radargram more resembles an inverted hyperbola.

Figure 7 shows the entire corrected GPR radargram produced from data collected at the Mock Rover site. Points A-C illustrate three such examples of hyperbolic subsurface reflections detected within the radargram. At these and other locations along

the transect, the hyperbolic reflectors are found immediately beneath the troughs as indicated by small V-shaped depressions in the stereo camera surface profile. Because polygon troughs are the most obvious surface expression of ice wedge locations [16], the successful coupling of our surface/subsurface model is further supported.

5 Conclusion and Future Work

We have presented a coupled surface/subsurface modeling method for planetary exploration. Our method uses only a stereo camera and a ground penetrating radar unit to produce:

1. An estimate of the rover's trajectory over the course of the traverse.
2. A photorealistic three-dimensional surface/subsurface model.
3. Topography-corrected GPR traces plotted with a two-dimensional profile of the surface along the transect.

The models and corrections allow operators to work remotely, surveying the data as if they were on site. Currently, there are several manual steps in terrestrial GPR site surveying. Our approach allows GPR collection to be carried out in an automated manner, on a rover, thereby enabling planetary exploration. Subsurface stratigraphy can be examined in the context of the surface morphology, a key scientific technique used by field geologists to identify sites worthy of further study.

We collected our data in a Mars analogue environment at sites of scientific interest. Visual odometry estimates were produced for approximately 800 meters of traverse. The coupled models were generated using only the types of sensors that are slated to fly on future rover missions, such as ExoMars.

As mentioned in Section 1, a flight rover's metal chassis and interference from the motors may corrupt the GPR signal. Our future work will include a return to Devon Island in July, 2009 to address this issue by direct comparison of GPR data collected with and without an actuated rover platform.

Acknowledgements Funding for this work was provided by The Canadian Space Agency's Canadian Analogue Research Network (CARN) program and the Natural Sciences and Engineering Research Council of Canada (NSERC). Gordon Osinski, Tim Haltigin, and Kevin Williams offered invaluable scientific guidance in the field and in production of the final data products. The Mars Institute and the Haughton-Mars Project provided infrastructure on Devon Island. Members of the communities of Resolute Bay, Grise Fjord, and Pond Inlet acted as guides, and protected us and our equipment from polar bears. Tom Lamarche from the Canadian Space Agency helped with our field testing. Peter Annan and David Redman from Sensors & Software Inc. helped us with equipment, and offered advice on the use of GPR in the field. Piotr Jasiobedzki and Stephen Se were instrumental in developing MDA Space Mission's Instant Scene Modeler and Ho-Kong Ng converted our motion estimates and images into surface models. Our algorithm used the SURF library developed by Herbert Bay, Luc Van Gool and Tinne Tuytelaars and available at <http://www.vision.ee.ethz.ch/surf/>.

References

1. Barfoot, T., D'Eleuterio, G., Annan, P.: Subsurface surveying by a rover equipped with ground penetrating radar. In: Proc. IEEE/RSJ Int. Conf. Intell. Robot. Syst. (IROS 2003), pp. 2541–2546. Las Vegas, NV (2003)
2. Barfoot, T., Se, S., Jasobedzki, P.: Visual Motion Estimation and Terrain Modelling for Planetary Rovers, chap. 4. Intelligence for Space Robotics. TSI Press, Albuquerque, NM (2006)
3. Barfoot, T.D.: Online visual motion estimation using fastslam with sift features. In: Proc. IEEE/RSJ Int. Conf. Intell. Robot. Syst. (IROS 2005), pp. 579–585 (2005)
4. Bay, H., Ess, A., Tuytelaars, T., Van Gool, L.: Speeded-up robust features (surf). Comput. Vis. Image Underst. **110**(3), 346–359 (2008). DOI <http://dx.doi.org/10.1016/j.cviu.2007.09.014>
5. Fischler, M.A., Bolles, R.C.: Random sample consensus: a paradigm for model fitting with applications to image analysis and automated cartography. Commun. ACM **24**(6), 381–395 (1981)
6. Folkesson, J., Christensen, H.: Sift based graphical slam on a packbot. In: Int. Conf. Field Serv. Robot. - FSR2007 (2007)
7. Fong, T., Allan, M., Bouysounouse, X., Bualat, M., Deans, M., Edwards, L., Fluckiger, L., Keely, L., Lee, S., Lees, D., To, V., Utz, H.: Robotics site survey at haughton crater. In: Proc. 9th Int. Symp. Artif. Intell., Robot. Autom. Space (iSAIRAS). Los Angeles, CA (2008)
8. Furgale, P., Barfoot, T., Ghafoor, N., Haltigin, T., Williams, K., Osinski, G.: Field testing of an integrated surface/subsurface modeling technique for planetary exploration (2008). In Preparation
9. Hinkel, K., Doolittle, J., Bockheim, J., Nelson, F., Paetzold, R., Kimble, J., Travis, R.: Detection of subsurface permafrost features with ground-penetrating radar, barrow, alaska. Permafrost and Periglac. Process. **12**, 179–190 (2001)
10. Howard, A.: Real-time stereo visual odometry for autonomous ground vehicles. In: Intell. Robot. and Syst., 2008. IROS 2008. IEEE/RSJ Int. Conf. on, pp. 3946–3952 (2008). DOI [10.1109/IROS.2008.4651147](https://doi.org/10.1109/IROS.2008.4651147)
11. Konolige, K., Agrawal, M., Solà, J.: Large scale visual odometry for rough terrain. In: Proc. Int. Symp. Res. Robot. (ISRR) (2007)
12. Kuzmin, R., Zabalueva, E.: Polygonal terrains on mars: Preliminary results of global mapping of their spatial distribution. In: Lunar and Planet. Sci. XXXIV, p. Abstract 1912 (2003)
13. Lachenbruch, A.: Mechanics of thermal contraction cracks and ice-wedge polygons in permafrost. Special paper to the Geological Society of America **70**, 69pp (1962)
14. Lowe, D.G.: Distinctive image features from scale-invariant keypoints. Int. J. Comput. Vis. **60**(2), 91–110 (2004)
15. Lunt, I.A., Bridge, J.S.: Evolution and deposits of a gravelly braid bar, Sagavanirktok river, Alaska. Sedimentol. **51**(3), 415–432 (2004)
16. Mackay, J.: Periglacial features developed on the exposed lake bottoms of seven lakes that drained rapidly after 1950, Tuktoyaktuk Peninsula area, Western Arctic coast, Canada. Permafrost and Periglacial Process. **10**, 39–63 (1999)
17. Maimone, M., Cheng, Y., Matthies, L.: Two years of visual odometry on the Mars Exploration Rovers. J. Field Robot. **24**(3), 169–186 (2007). Maimone, Mark Cheng, Yang Matthies, Larry
18. Matthies, L.: Dynamic stereo vision. Ph.D. thesis, Carnegie Mellon University Computer Science Department (1989). Chairman-Steven A. Shafer
19. Nistér, D., Naroditsky, O., Bergen, J.: Visual odometry. Proc. 2004 IEEE Comput. Soc. Conf. Comput. Vis. Pattern Recognit. (CVPR 2004) **01**, 652–659 (2004)
20. Nistér, D., Naroditsky, O., Bergen, J.: Visual odometry for ground vehicle applications. J. Field Robot. **23**(1), 3 (2006)
21. Se, S., Jasobedzki, P.: Stereo-vision based 3d modeling and localization for unmanned vehicles. Int. J. Intell. Control Syst. **13**(1), 47–58 (2008). Special Issue on Field Robotics and Intelligent Systems
22. Vago, J., Gardini, B., Kmínek, G., Baglioni, P., Gianfiglio, G., Santovincenzo, A., Bayón, S., van Winnendaal, M.: ExoMars - searching for life on the Red Planet. ESA Bull. **126**, 16–23 (2006)